Cytotechnology (2021) 73:657–667
https://doi.org/10.1007/s10616-021-00486-z

ORIGINAL ARTICLE

Altered properties of human adipose-derived mesenchymal stromal cell during continuous in vitro cultivation

Lianhua Jin · Na Lu · Wenxin Zhang · Yan Zhou

Received: 6 December 2020 / Accepted: 5 July 2021 / Published online: 9 July 2021

Abstract Adipose-derived stromal cells (ASCs) are now recognized as an accessible, abundant, and reliable stem cells for tissue engineering and regenerative medicine. However, ASCs should be expanded long term in order to harvest higher cell number for clinical application. In this study, ASCs isolated from human subcutaneous adipose tissue and senescence after long-term expansion was evaluated. The results showed that following in vitro expansion to the 15th passage, ASCs show changes in morphology (toward the "fried egg" morphology) and decrease in proliferation potential. Nonetheless, ASCs maintained differentiation potential toward osteoblasts, chondrocytes, and adipocytes. The senescent ASCs show impaired migration capacity under the same basal conditions. OXPHOS and glycolysis decreased slightly in culture from passage 5 to passage 15. ASCs also showed increased accumulation of beta-galactosidase in culture. Expression of senescence markers p53, p16, and p21 were also increased accompanied with the increase of passages. Experiment data showed that ASCs biological characteristics depended and changed with age. We recommend the use of early-passage cells, particularly those before passage 5, for efficacious therapeutic application of stem cells.

Keywords Adipose derived mesenchymal stromal cells · Senescence · Mitochondrial energy metabolism · Glycolysis · Proliferation

L. Jin · N. Lu · Y. Zhou (✉)
Pediatric Cardiovascular Department, The First Hospital of Jilin University, Jilin, China
e-mail: zhou_y@jlu.edu.cn

W. Zhang
School of Clinical Medicine, Jilin University, Jilin, China

Introduction

Mesenchymal stromal cells (MSCs) is a pluripotent stem cell with multi-directional differentiation potential, self-renewal and high proliferation capacity. At present, researches are focused on bone marrow mesenchymal stromal cells (BM-MSCs) (Estrada et al. 2013). Compared with embryonic stem cells, BM-MSCs does not involve ethical tissue, but the harvest of bone marrow may cause damage to donor, which limits its application (Samih et al. 2018). Adipose derived mesenchymal stromal cells (ASCs) have biological characteristics similar to BM-MSCs, and high amounts of ASCs with minimal invasiveness are easily accessible (Gimble et al. 2011).Therefore, ASCs are considered as a perspective tool in cell therapy and regenerative medicine, becoming a potential substitute for BM-MSCs (Fraser et al. 2006).ASCs are isolated from liposuction fat for the first time by Zuk et al. (2001).and cell therapy of ASCs has been used in several human clinical trials, such as soft tissue augmentation (Zhou et al. 2011), idiopathic

pulmonary fibrosis (Tzouvelekis et al. 2013), myocardial ischemia (Murohara et al. 2009), and osteoarthritis (Freitag et al. 2019).

In order to obtain sufficient ASCs for clinical application, long-term cell expansion are indispensable. Primary cells are continuously subcultured in vitro, which ultimately leads to replicative senescence and eventually die through apoptosis. The senescence of ASCs which manifests as morphological senescence, reduced proliferation and differentiation potential, increased senescence–associated β-galactosidase (SA-β-Gal) activity, deranged mitochondrial metabolism, altered immunoregulation are found during the cultivation in vitro, which profoundly affects clinical application (Seok et al. 2020; Eduardo et al. 2020; Sethe et al. 2006; Boyette and Tuan 2014). Although a 3D suspension culture system by using spinner flasks added with microcarrier has been reported (Carmelo et al. 2015), less is known about ASCs expansion and senescence. Obtaining mass production of high-quality ASCs and maintaining the biological characteristics during expansion has become an important tissue (Liu et al. 2017a).

The aim of this study was to systematically investigate the characteristics of senescent ASCs after long-term expansion in vitro, including cell morphology, senescent properties, mult-differentiation potential, and migration ability, with special emphasis on their energy metabolism. The results provided new insight into the extent of aging and limitations of multiple passages of culture, underlying the replicative senescence related decline of the therapeutic potential of stem cells.

Results and discussion

ASCs changed in shape and proliferation

ASCs are ideal target cells for tissue and genetic engineering, the clinical application of ASCs have been widely studied for many diseases (Salem and Thiemermann 2010). Gimble (Blanc and Mougiakakos 2012) proposed that stem cells must have enough cells (million to billions) for clinical application. In the body, the quantity of ASCs is not high. After separation from the source, cells must be cultured to provided sufficient number of high-quality cells for therapeutic purpose (Mosna et al. 2010). Numerous studies have shown that the characteristics of ASCs may alter during prolonged culturing (Hladik et al. 2019; Gu et al. 2016; Truong et al. 2019).

Firstly, the morphology change and proliferation capacity of ASCs were recorded. ASCs were cultured and continuously subcultured to passage 5, passage 10, and passage 15. At passage 5, cells had the characteristic spindle-shaped, smooth cell surface and grew regularly. At passage 10, the cells maintained the characteristic ASCs shape. Some cells were polygonal, became long and flat. Unlike ASCs at passage 5, almost all ASCs at passage 15 exhibited star-shaped with pseudopods, and become larger and flatter (Fig. 1D). As well, morphology change of ASCs from spindle-shaped to star-shaped at passage 15 were confirmed by hematoxylin staining (Fig. 1E). In addition to morphology change, cell growth curve revealed a slight trend toward decreasing in proliferation rate accompanied with passage increasing (Fig. 1A). For further evaluation the self-renewal capacity of ASCs, we measured and calculated CPDL. The results showed that CPDL of P5, P10, P15 ASCs were (8.15 ± 1.48) h, (13.90 ± 2.62) h and (31.24 ± 3.21) h, respectively. ASCs morphology and proliferation capacity change was consistent with report by Wagner et al. (2019), which suggests that after long time cultivation outside the body, ASCs increase in size, flattened, and lost their ability to proliferate.

The cell cycle distribution of ASCs was detected by FACS analysis. At passage 15, the percentage of G1 cells was significantly increased up to $(87.86 \pm 5.46)\%$, indicating G1 arrest, compared to passage 5 $(80.26 \pm 4.28)\%$ and passage 10 $(85.33 \pm 6.28)\%$, even though there were no difference in the percentage of sub-G1 cells among different passages. Concomitant with this, the percentages of cells in S populations were reduced from $(12.28 \pm 1.86)\%$ (passage 5) to $(10.04 \pm 1.92)\%$ (passage 10) and $(5.5 \pm 1.02)\%$ (passage 15), respectively. There were significant difference in the percentage of S phase cells in different passages ($P < 0.05$) (Fig. 1B). An assessment of the percentage of cells in live, apoptotic, and dead status among the ASCs, a slight increase in the number of cells in apoptotic status at the passage 15 compared with the other 2 passages was observed (Fig. 1C).

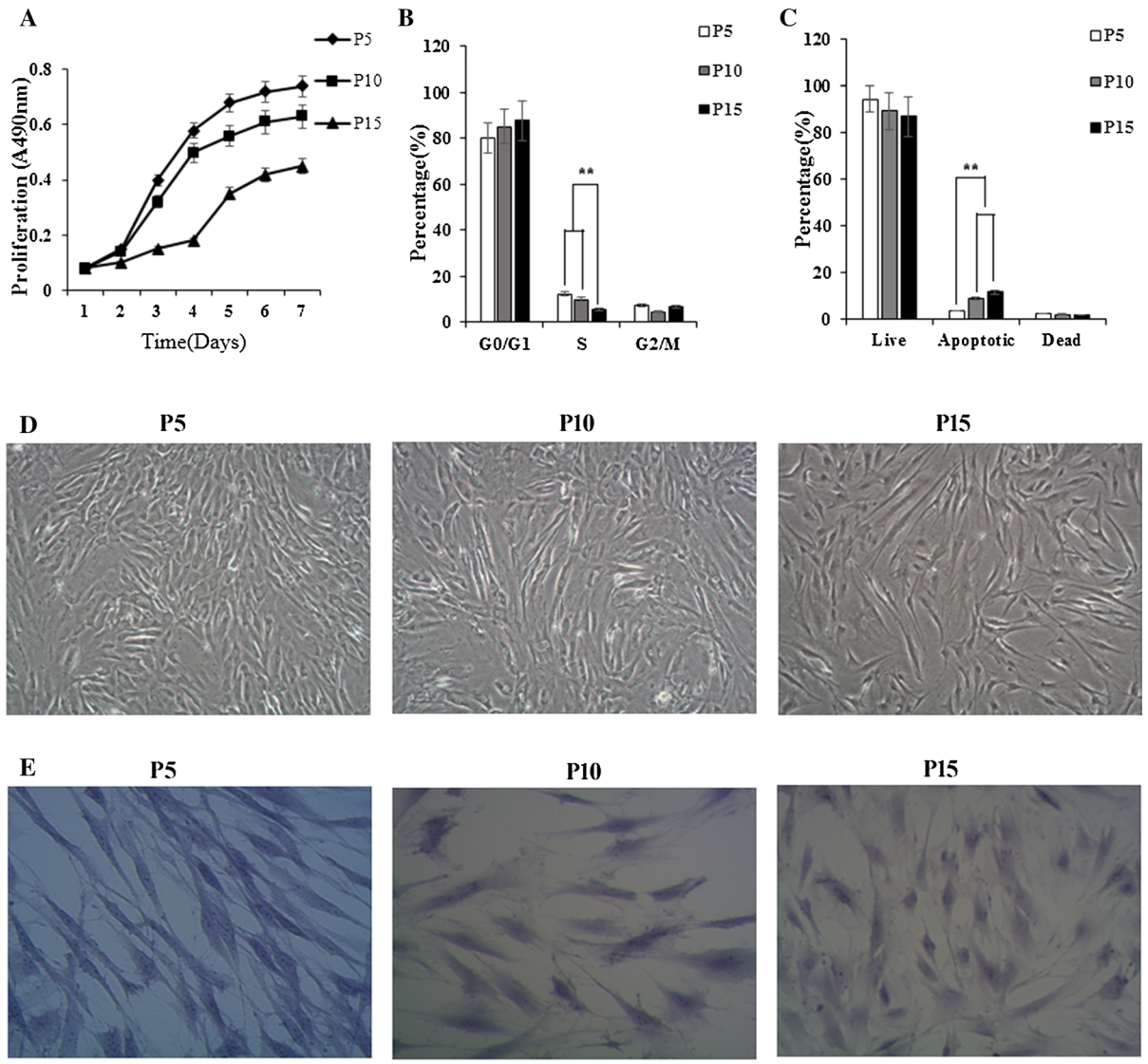

Fig. 1 Characterization of senescent ASCs during long-term cultivation. **A** Different passage ASCs growth curve. Cells growth curve revealed a slight trend toward decreasing in proliferation capacity accompanied with passage increasing. **B** Cell cycle analyzed by FACS analysis. There were significant difference in the percentage of S phase cells in different passages ($P < 0.05$). **C** Apoptosis was analyzed using a Muse Cell Analyzer. A slight increase in the number of cells in apoptotic status at the passage 15 compared with the other 2 passages was observed. **D** Morphological change of ASCs (magnification, ×100). Passage 5 ASCs had spindle-shaped, smooth cell surface and grew regularly. Passage 10 ASCs were polygonal, became long and flat. Passage 15 ASCs become larger and flatter. **E** HE staining of ASCs (magnification, ×200). The enlarged cell size was significantly observed in passage 15 ASCs by HE staining

Change in trilineage differentiation

Truong et al. (2019); Wagner et al. (2019) report ASCs retained the potential to differentiate into adipocyte, osteogensis and chondroblast from passage 5 to passage 15. However, Seo et al. (2020) reported that ASCs lost their self-renewal and multi-differentiation potent during long time cultivation in vitro. The multilineage differentiation potential of ASCs were necessary to examine undergoing secondary culture. ASCs were seeded in 6-well plates with homogeneous density and induced to differentiate into adipocyte, osteogensis and chondroblast. The results showed that despite several generations of subculturing (up to

passage 15), ASCs retained their ability to differentiate into the three specific cell lines. However, at passage 15, cell density was less than the early passages and the space between cells increased remarkably (Fig. 2).The results is inconsistent with some reports (Baer et al. 2010).

Change in migration ability

In the clinical application of ASCs transplantation, the tissue repairing process is also affected by the capacity of ASCs to migrate to the injured organ (Liu et al. 2017b). Martha et al. found that, compared with young BM-MSCs, the migration capacity and soluble factors expression of aged BM-MSCs were significantly reduced (Arango-Rodriguez et al. 2015). The migration ability of ASCs were detected by scratch test and transwell system (Cardenes et al. 2018). The results of the scratch test showed that the migration ability of ASCs was significantly decreased with culture time (Fig. 3A). Furthermore, the transwell assay revealed that the number of migratory cells of passage 15 was remarkably reduced compared to passage 5 and 10 within 24 h (Fig. 3B). Therefore, we conclude that the senescent ASCs show an impaired migration capability under the same basal conditions. With sequential passages, the proliferation and migration potential of ASCs decreases greatly, which will affect the efficacy of stem cell therapy (Lee et al. 2018).

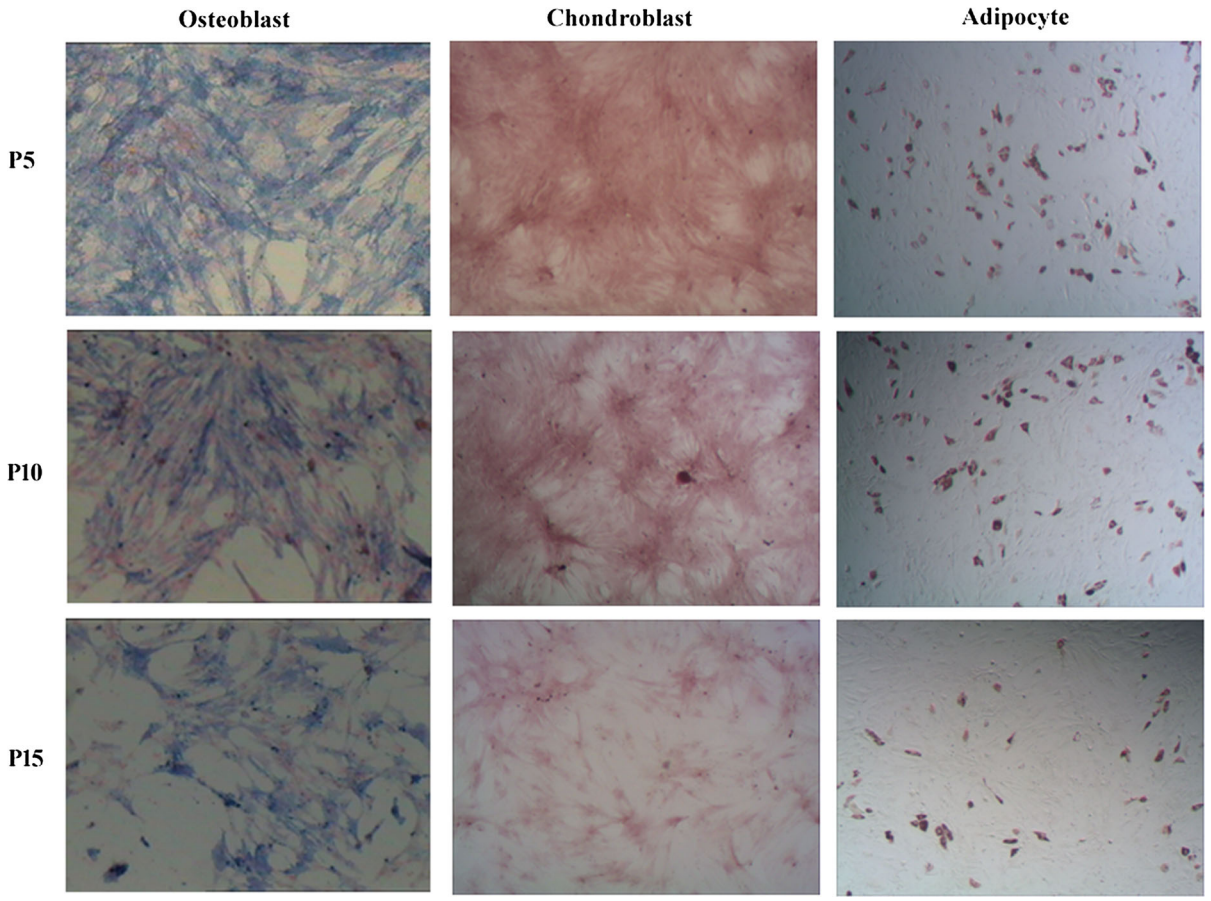

Fig. 2 Trilineage differentiation capacity of ASCs in vitro (magnification, ×100). Over 15 passages of subculture, ASCs have retained the ability to differentiate into adipocyte, osteogensis and chondroblast. Passage 15 cell density was less than the early passages and the space between cells increased remarkably

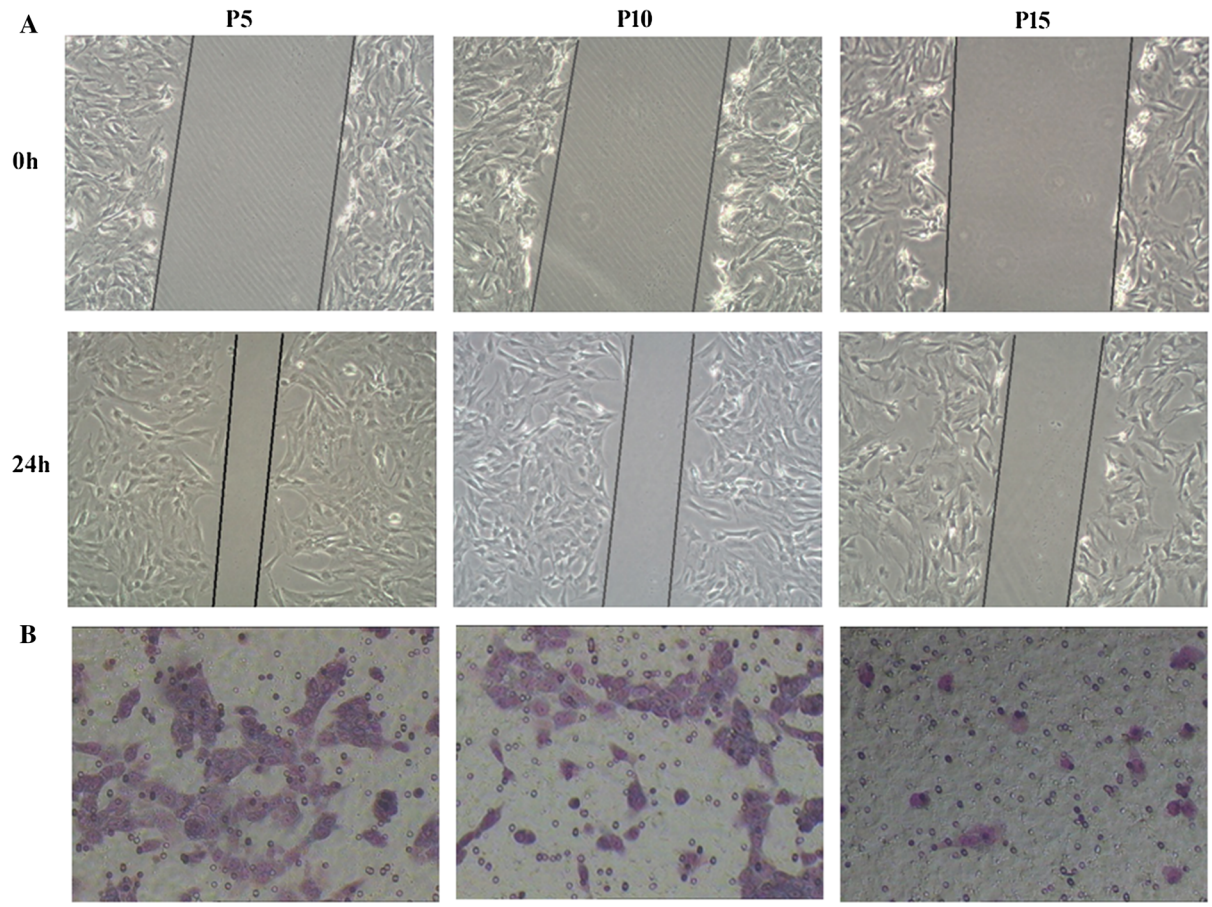

Fig. 3 The migration ability of ASCs (magnification, ×100). **A** Images from the scratch wound migration assay. Healing due to the cellular migration of ASCs was observed over a period of 24 h following scratch wounding. The results showed that the migration ability of ASCs was significantly decreased with culture time. **B** Representative images of cell migration using a transwell assay. The transwell assay revealed that the number of migratory cells of passage 15 was remarkably reduced compared to passage 5 and 10 within 24 h

OXPHOS and glycolysis impaired at senescence ASCs

After determining that proliferation capacity is altered with cultivation time, we next detected whether ASCs metabolism is impacted during long-term expansion. We measured both OCR and ECAR to evaluate mitochondrial oxidative phosphorylation function and cellular glycolysis function under baseline and stressed (stimulated to maximize energy production) conditions (Figs. 4A, 5A). For baseline OCR and spare respiratory capacity revealed that within passage 15, passage 15 had moderately lower baseline OCR and spare respiratory capacity when compared to passage 5 and 10 ($P < 0.05$) (Fig. 4B). We observed that passage 15 had a significantly lowed maximal respiration and ATP production when compared to passage 5 and passage 10 ($P < 0.05$) (Fig. 4C). For glycolysis, the results displays that passage 15 had lower glycolysis and glycolytic capacity compared to passage 5 and 10 ($P < 0.05$).Glycolytic reserve was not significantly different between passage 5, 10 and 15 ASCs (Fig. 5B). The results showed that early ASCs had a significantly greater OCR metabolic potential, suggesting senescent ASCs used less of OXPHOS capacity during expansion. The results is consistent with others reports (Ji et al. 2019). Results from our study suggest that ASCs glycolysis function was maintained, however there was slightly reduced in passage 15 ASCs.

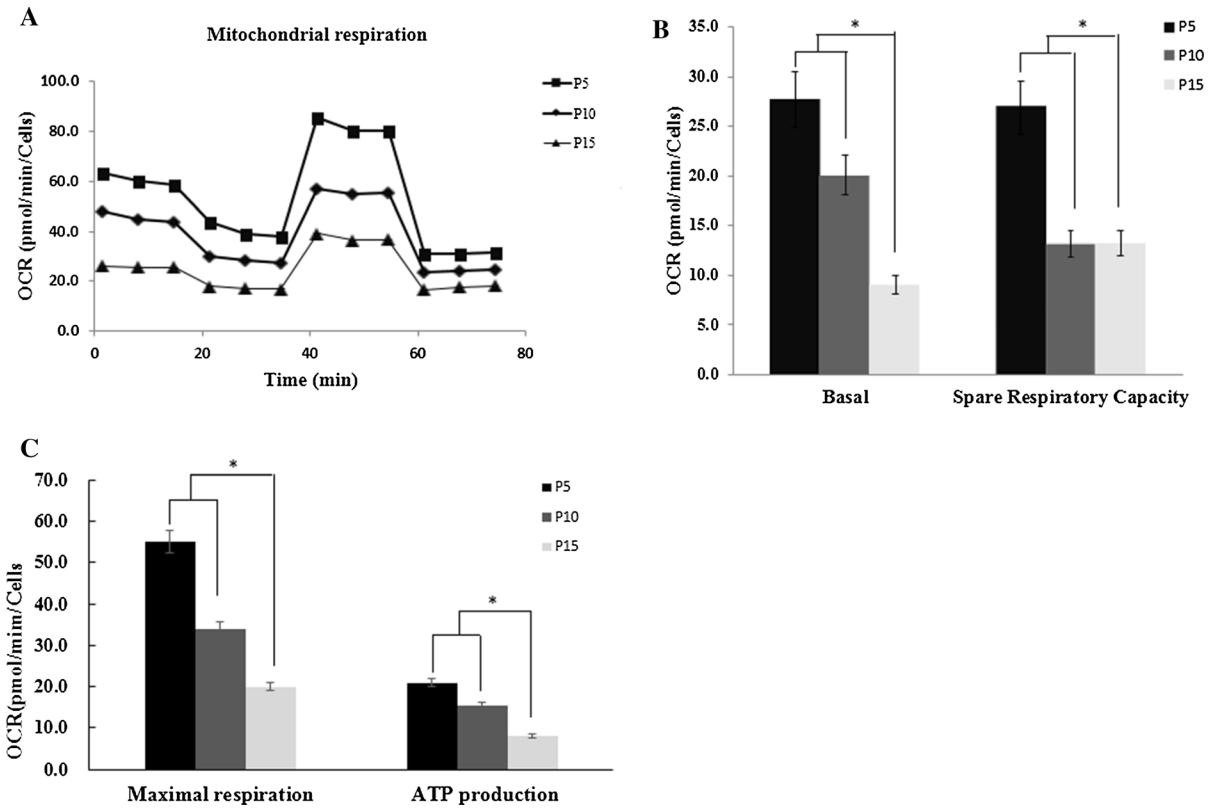

Fig. 4 Oxygen-consumption rate (OCR) indicates lower oxidative metabolism in senescence ASCs. **A** The curve of different passage ASCs mitochondrial stress test. **B** Passage 5, 10 and 15 ASCs basal respiration and spare respiratory capacity. Passage 15 ASCs had moderately lower baseline OCR and spare respiratory capacity when compared to passage 5 and 10 ($P < 0.05$). **C** Passage 5, 10 and 15 ASCs maximal respiration and ATP production. Passage 15 had a significantly lowed maximal respiration and ATP production when compared to passage 5 and passage 10 ($P < 0.05$)

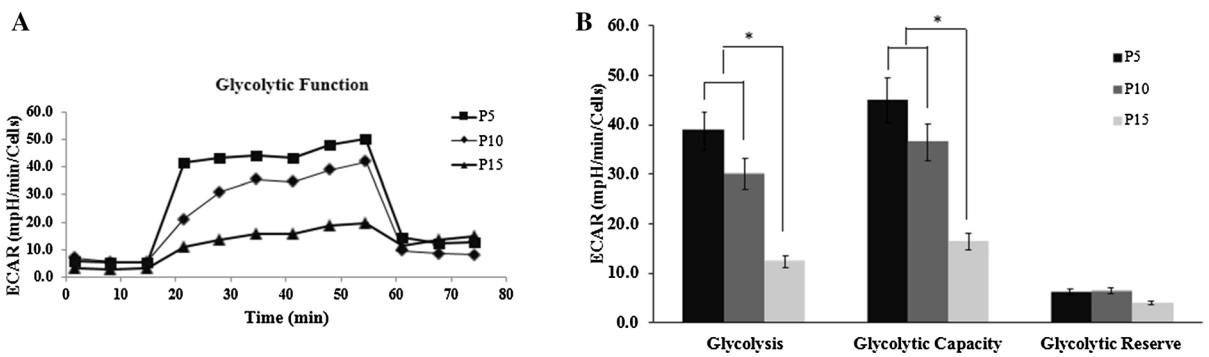

Fig. 5 Extracellular acidification rate (ECAR) indicates lower glycolysis in senescence ASCs. **A** The curve of different passage ASCs glycolysis stress test. **B** Passage 5, 10 and 15 ASCs glycolysis, glycolytic capacity and glycolytic reserve. Passage 15 ASCs had lower glycolysis and glycolytic capacity compared to passage 5 and 10 ($P < 0.05$). Glycolytic reserve was not significantly different between different passage ASCs

Elevated cell senescence with increasing passages

Finally, the senescence of ASCs at different passages was examined using SA-β-gal staining. SA-β-gal activity is the most commonly used biomarker for the identification of senescent cells. The senescent status of ASCs were confirmed by the SA-β-gal staining assay showing an increased activity of the lysosomal β-galactosidase specifically in senescent cells. Many senescent ASCs, which were large and flat in shape and showed aquamarine in cytoplasm after SA-β-gal staining. We observed a significant increase in SA-β-gal-positive cells with increasing culture time (Fig. 6A). At passage 15, SA-β-gal-positive cells were increased up to (52.4 ± 5.8)%, compared to passage 5(3.8 ± 0.8)% and passage 10 (15.3 ± 1.2)%, there were significantly difference ($P < 0.05$) (Fig. 6B). The results were similar to the results of Legzdina et al. (2016). To evaluate senescence at the molecular level, we also monitored the level of cellular senescence-related proteins p53, p21 and p16 at different passages. The senescence markers p53, p16, and p21 were also increased accompanied with the increase of passage (Fig. 6C). This result suggests that ASCs are replicative senescence during in vitro amplification.

Experimental section

Isolation and primary culture of ASCs

The fat tissue was obtained from healthy patients undergoing abdominal surgery (age range of 22–27 years; $n = 3$). All patients provided written informed consent for research use of tissues and for publication. Ethical approval was also obtained from the Research Ethics Committee of the First Clinical Hospital of Jilin University.

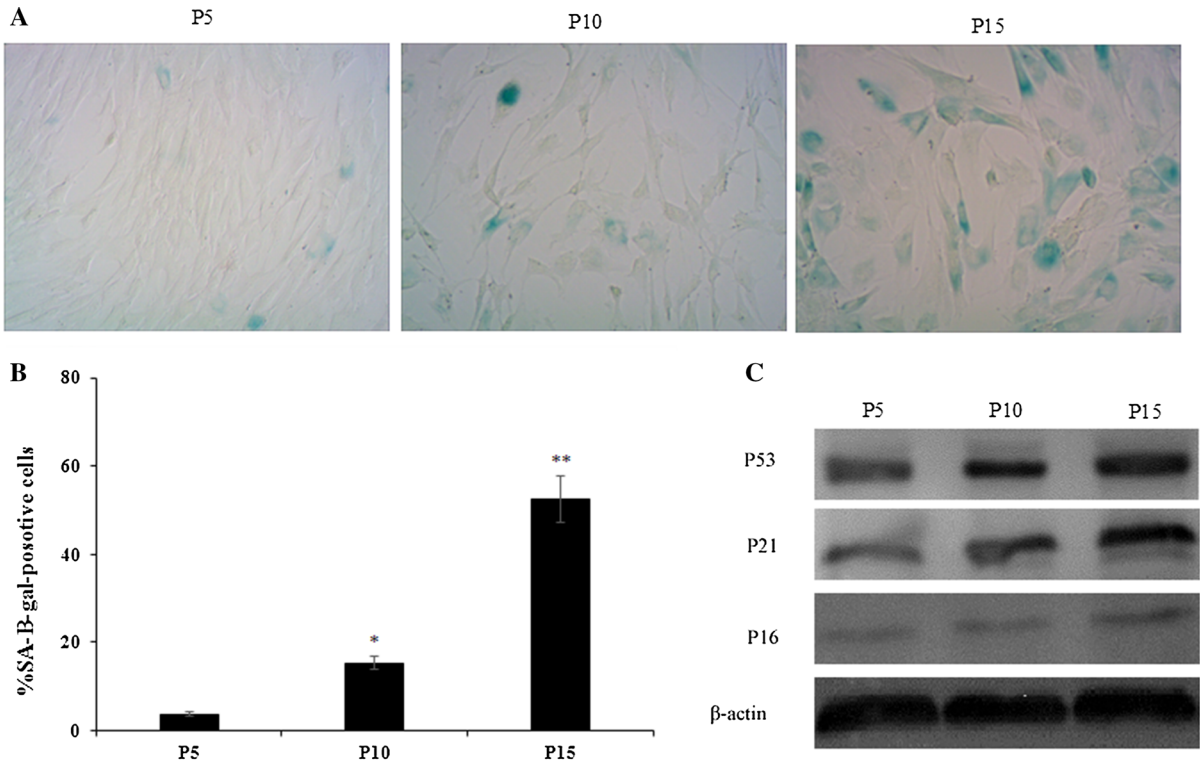

Fig. 6 Characterization of ASCs replicative senescence. **A** Representative images of SA-β-gal -positive ASCs at different passages (magnification, ×200). Many senescent ASCs, which were large and flat in shape and showed aquamarine in cytoplasm after SA-β-gal staining. **B** Percentage of SA-b-gal-positive ASCs at different passages. The results showed a significant increase in SA-β-gal-positive cells with increasing culture time. **C** Representative images of western blot for p53, p21 and p16 protein levels of different passage ASCs sample. The senescence markers p53, p16, and p21 were increased accompanied with the increase of passage

ASCs were isolated and cultured as previously described (Iyyanki et al. 2015).The fat tissue was washed 3 times with phosphate-buffered saline (PBS), and digested with 0.1% (w/v) type I collagenase (Sigma-Aldrich, St Louis, MO, USA) at 37 °C for 45 min with gentle agitation. Undigested tissues and unneeded oils were filtered out using a screen mesh followed by centrifugation at 1500 rpm for 5 min, and the final pellet was resuspended in complete culture media consisting of Dulbecco's modified Eagle's medium(DMEM, Gibco, USA), 10% fetal bovine serum(FBS, HyClone, South, Logan, UT, USA), and 0.1% penicillin (Cyagen Biosciences, Guangzhou, China). Finally, cells were plated at a density of 1.5×10^5 cells/cm^2 for culture in fresh complete medium in a humidified 37 °C incubator with 5% CO_2. Forty-eight hours after isolation, unattached cells were washed off, and the medium was changed every 3 days.

ASCs expansion

ASCs samples from primary culture were subcultured with Trypsin/EDTA, 0.25% (Corning, NY, USA), and then cultured in complete medium at 37 °C in a humidified atmosphere set at 5% CO_2. The cells were passaged when cell density reached 90% confluency (up to passage 15). To analyze the characteristics of in vitro senescent ASCs during long-term cultivation, we compared differences in various biological characterization related to senescence at passages 5, 10 and 15.

Cell proliferation

The proliferation and growth efficiency of ASCs were determined by MTS assay and cumulative population doubling level (CPDL) assay. MTS assay is a colorimetric assay with 3-(4,5-dimethylthiazol-2-yl)-5-(3-carboxymethoxyphenyl)-2-(4-sulfophenyl)-2H-tetrazolium (MTS) (Promega, Madison, WI, USA) following the manufacturer's instructions. In brief, MSCs was seeded into 96-well plate (4×10^3cells/well) (Corning, NY, USA) and cultured for 1, 2, 3,4, 5, 6,7 days, then 20 μL of MTS solution was added to each well and incubated for 4 h at 37 °C. The absorbance was measured by an Epoch microplate spectrophotometer (Biotek, VT, USA) at 490 nm. CPDL assay (Seo et al. 2021) using the formula CPDL = ln (Nf/Ni) ln2, where Ni is the initial seeding cell number, Nf is the final harvest cell numbers, and ln is the natural log. Each assay was performed in three replicate wells for each condition.

Cell cycle assays

Cell cycle analysis kit (Beyotime Institute of Biotechnology, Beijing, China) was used for cell cycle following the manufacturer's instructions. In brief, 1×10^6 ASCs were centrifuged and washed with PBS for three times, then fixed in 70% ice cold ethanol at − 20 °C overnight. Cells were resuspended in 1 ml cold PBS containing RNase (50 μg/ml), then stained with propidium iodide (PI; 5 μg/ml) for 30 min at room temperature in the dark. The cell cycle was analyzed using BD FACS Vantage SE Cell Sorter (BD Bioscience Pharmingen, San Diego, CA, USA).

Apoptosis assay

A Muse Cell Analyzer was used for apoptosis studies using the Muse Annexin V& Dead Cell Assay. Cells were harvested, washed with PBS for three times, and incubated with Annexin V binding buffer according to the manufacturer's instructions. The percentage of normal, apoptotic, and necrotic cells was analyzed with Muse Cell Analyzer (Millipore, Billerica, MA, USA).

Assessment of trillineage differentiation

The adipocyte, osteogensis and chondroblast differentiation capabilities of ASCs were performed using Oricell adipogenesis differentiation kit (Cyagen Bioscience, China), Oricell chondrogenic differentiation kit (Cyagen Bioscience, China) and Oricell Osteogenic Differentiation kit (Cyagen Bioscience, China), respectively. ASCs were cultured in 6-well plates (Corning, NY, USA) and were supplemented with respective differentiation medium upon reaching 90% confluent. The inductive medium was changed every 3 days for 21 days. For adipogenic induction, lipid droplets were detected by Oil Red O (Sigma-Aldrich) staining. For osteogenesis differentiation, cells were detected by Alkaline phosphatase staining, (Cyagen Bioscience, China) following the manufacture instructions, whereas for chondroblast differentiation, cells

were stained with Safranin O (Cyagen Bioscience, China).

ASCs migration ability assays

A scratch test and a transwell assay were used to determine the change in the migration ability of MSCs. The scratch test were performed according to previously reported (Liang et al. 2007). Briefly, 5×10^5 cells were seeded into the 6-well plates (Corning, NY, USA). After 24 h, cell scratches were made with a 200-μL pipette tip, and residual cells were washed with PBS for three times. DMEM containing 1% FBS was used to culture cells for 24 h. The healing condition of the cells were photographed by Olympus CKX41 microscope. Transwell assays were performed using an 8-μm pore size transwell chamber in 24-well plates (Corning, NY, USA). Cells were plated in the upper chamber of the transwell at a density of 2.5×10^5 cells/mL, cultured with DMEM containing 1% FBS. At the same time, DMEM containing 20% FBS was added in the lower chamber. After 24 h, migrated cells appeared in the lower side of the transwell membrane and were fixed with 4% neutral formaldehyde 30 min and stained with 0.1% crystal violet.

Seahorse analysis of mitochondrial respiration and glycolysis

The seahorse bioscience extracellular flux analyzer (Seahorse Bioscience, Billerica, MA, USA) was used to monitor OCR (oxygen consumption rate) and extracellular acidification rate (ECAR) to detect cellular OXPHOS and glycolysis. Experiments were performed according to the manufacturer's instructions. OCR and ECAR were measured using Seahorse XF Cell Mito Stress Test Kit and Seahorse XF Glycolysis Stress Test Kit, respectively. Briefly, cells were seeded in a Seahorse XF cell culture microplate at a density of 1.5×10^4 per well. For OCR, oligomycin, the reversible inhibitor of oxidative phosphorylation FCCP (p-trifluoromethoxy carbonyl cyanide phenylhydrazone), and the mitochondrial complex I inhibitor rotenone plus the mitochondrial complex III inhibitor antimycin A (Rote/AA) were sequentially injected; and for ECAR, after baseline measurements, glucose, the oxidative phosphorylation inhibitor oligomycin, and the glycolytic inhibitor 2-DG were sequentially injected into each well at indicated time points. According to the OCR value, the basic respiration, maximum respiration, respiration capacity and ATP production (ATP production) were analyzed. According to the ECAR value, the glycolysis, glycolytic capacity and glycolytic reserve were analyzed. OCR and ECAR were normalized according to cell number (1×10^4).

SA-β-galactosidase assays

5×10^5 cells were seeded in a 6-well plate in triplicates. After 48 h, senescence-associated β-galactosidase (SA-β-gal) staining was performed using a β-galactosidase Staining Kit (Beyotime, Shanghai, China) according to the manufacturer's instructions. Briefly, ASCs were washed with PBS and fixed using the fixative solution for half an hour at room temperature and then incubated at 37 °C overnight with the SA-β-gal staining solution. The senescent ASCs stained with blue were photographed by Olympus CKX41 microscope. The percentage was calculated from five different view fields of each sample in three independent experiments.

Western blotting

The proteins of different passage ASCs were extracted and the concentrations measured. A total of 15 μg protein from each sample was loaded, electrophoresed on 12.5% SDS-PAGE gels and then transferred to a PVDF membrane. Membranes were sequentially incubated with the following antibodies at 4 °C overnight at an appropriate dilution (1:1000): mouse anti-P53(Pab240, SC-99, Santa Cruz Biotech, CA, USA), anti-P21 (F5, SC-6246,Santa Cruz Biotech, CA, USA), anti-P16 (F-12, SC-1661, Santa Cruz Biotech, CA, USA),and anti-β-actin (SC-137179, Santa Cruz Biotech, CA, USA). Subsequently the membrane was washed with TBST for 0.5 h and then incubated with horseradish peroxidase-conjugated secondary antibodies (1: 2000; Santa Cruz Biotech, CA, USA) at room temperature for one hour. Specific complexes were visualized using Electro-Chemi-Luminescence (ECL) detection kit (Tanon Biotech, Shanghai, China) following the manufacturer's instructions.

Data analysis

Data are presented as mean ± standard deviation (SD). For quantitative analysis of the differences among the mean values between the groups, data were analyzed using one-way analysis of variance (ANOVA) with Turkey's post hoc multiple comparison test through GraphPad Prism software. All experiments were performed at least in triplicate. A value of $P < 0.05$ was considered statistically significant.

Conclusion

In the present study, we confirmed the changes in the characteristics of ASCs that occurred with long-term cultivation in medium containing FBS in vitro. We observed a continuous decrease in the self-renewal ability, migration capacity, mitochondrial OXPHOS function, and glycolysis function of these cells over subsequent passages during in vitro culture, significant differences in the expression of cellular senescence-related proteins p53, p21 and p16, which commenced at passage 10 and passage 15. Culture medium is the key to the efficiency and safety of ASCs and needs to be able to maintain the phenotype, function and gene stability of ASCs after continuous subculture. Clinical gra7de ASCs requires safety products to replace FBS, such as human serum, platelet lysate or chemically defined GMP medium. We are observing the changes in the biological characteristics of ASCs after long-term in medium containing human serum in vitro.

Acknowledgements The work was supported by Jilin Provincial Development and Reform Commission (2016C042-2) and Health Department of Jilin Province (2020J122).

Declarations

Conflict of interest The authors have no conflicting financial interest.

References

Arango-Rodriguez ML, Ezquer F, Conget P et al (2015) Could cancer and infection be adverse effects of mesenchymal stromal cell therapy? World J Stem Cells 7:408–417

Baer PC, Gresche N, Luttmann W et al (2010) Human adipose-derived mesenchymal stem cells in vitro: evaluation of an optimal expansion medium preserving stemness. Cytotherapy 12:96–106

Boyette LB, Tuan RS (2014) Adult stem cells and diseases of aging. J Clin Med 3:88–134

Cardenes N, Alvarez D, Sellares J et al (2018) Senescence of bone marrow-derived mesenchymal stem cells from patients with idiopathic pulmonary fibrosis. Stem Cell Res Ther 9:257

Carmelo JG, Fernnandes-Platzgummer A, Diogo MM et al (2015) A xeno-free microcarrier-based stirred culture system for the scalable expansion of human mesenchymal stem/stromal cells isolated from bone marrow and adipose tissue. Biotechnol J 10:1235–1247

Eduardo FR, Julia F, Roman G et al (2020) Senescence-associated metabolomic phenotype in primary and iPSC-derived mesenchymal stromal cells. Stem Cell Reports 14:201–209

Estrada JC, Torres Y, Benguria A et al (2013) Human mesenchymal stem cell-replicative senescence and oxidative stress are closely linked to aneuploidy. Cell Death Dis 4:e691

Fraser JK, Wulur I, Alfonso Z et al (2006) Fat tissue: an underappreciated source of stem cells for biotechnology. Trends Biotechnol 24:150–154

Freitag J, Bates D, Wickham J et al (2019) Adipose-derived mesenchymal stem cell therapy in the treatment of knee osteoarthritis: a randomized controlled trial. Regen Med 14:213–230

Gimble JM, Bunnell BA, Floyd ZE (2011) Prospecting for adipose progenitor cell biomarkers: biopanning for gold with in vivo phage display. Cell Stem Cell 9:1–2

Gu Y, Li T, Ding Y, Sun L et al (2016) Changes in mesenchymal stem cells following long-term culture in vitro. Mol Med Rep 13:5207–5215

Hladik D, Höfig I, Oestreicher U, Beckers J et al (2019) Long-term culture of mesenchymal stem cells impairs ATM-dependent recognition of DNA breaks and increases genetic instability. Stem Cell Res Ther 10:218

Iyyanki T, Hubenak J, Liu J et al (2015) Harvesting technique affects adipose-derived stem cell yield. Aesthet Surg J 35:467–476

Ji J, Fu T, Dong C et al (2019) Targeting HMGB1 by ethyl pyruvate ameliorates systemic lupus erythematosus and reverses the senescent phenotype of bone marrow-mesenchymal stem cells. Aging 11:4338–4353

Le Blanc K, Mougiakakos D (2012) Multipotent mesenchymal stromal cells and the innate immune system. Nat Rev Immunol 12:383–396

Lee BY, Li Q, Song WJ et al (2018) Altered properties of feline adipose-derived mesenchymal stem cell during continuous in vitro cultivation. J Vet Med Sci 80:930–938

Legzdina D, Romanauska A, Nikulshin S et al (2016) Characterization of senescence of culture-expanded human adipose-derived mesenchymal stem cells. Int J Stem 9:124–136

Liang CC, Park AY, Guan JL (2007) In vitro scratch assay: a convenient and inexpensive method for analysis of cell migration in vitro. Nat Protoc 2:329–333

Liu MC, Lei H, Dong P et al (2017a) Adipose-derived mesenchymal stem cells from the elderly exhibit decreased

migration and differentiation abilities with senescent properties. Cell Transplant 26:1505–1509
Liu M, Lei H, Dong P (2017b) Adipose-derived mesenchymal stem cells from the elderly exhibit decreased migration and differentiation abilities with senescent properties. Cell Transplant 26:1505–1519
Mosna F, Sensebe L, Krampera M (2010) Human bone marrow and adipose tissue mesenchymal stem cells: a user's guide. Stem Cells Dev 19:1449–1470
Murohara T, Shintani S, Kondo K (2009) Autologous adipose-derived regenerative cells for therapeutic angiogenesis. Curr Pharm Des 15:2784–2790
Salem HK, Thiemermann C (2010) Mesenchymal stromal cells: current understanding andclinical status. Stem Cells 28:585–596
Samih MA, Inge F, Stein AL et al (2018) Adipose-derived and bone marrow mesenchymal stem cells: a donor-matched comparison. Stem Cell Res Ther 9:168
Seo Y, Shin TH, Ahn JS et al (2020) Human tonsil-derived mesenchymal stromal cells maintain proliferating and ROS-regulatory properties via stanniocalcin-1. Cells 9:636
Seo MS, Kang KK, Oh SK et al (2021) Isolation and characterization of feline Wharton's jelly-derived mesenchymal stem cells. Vet Sci 8:24
Seok J, Jung HS, Park S et al (2020) Alteration of fatty acid oxidation by increased CPT1A on replicative senescence of placenta-derived mesenchymal stem cell. Stem Cell Res Ther 11:1
Sethe S, Scutt A, Stolzing A (2006) Aging of mesenchymal stem cells. Ageing Res Rev 5:91–116
Truong NC, Bui KH, Van Pham P (2019) Characterization of senescence of human adipose-derived stem cells after long-term expansion. Adv Exp Med Biol 1084:109–128
Tzouvelekis A, Paspaliaris V, Koliakos G et al (2013) A prospective, non-randomized, no placebocontrolled, phase Ib clinical trial to study the safety of the adipose derived stromal cells-stromal vascular fraction in idiopathic pulmonary fibrosis. J Transl Med 11:171
Wagner DR, Karnik S, Gunderson ZJ et al (2019) Dysfunctional stem and progenitor cells impair fracture healing with age. World J Stem Cells 11:281–296
Zhou YL, Yan ZW, Zhang HM et al (2011) Expansion and delivery of adipose-derived mesenchymal stem cells on three microcarriers for soft tissue regeneration. Tissue Eng Part A 17:1981–1997
Zuk PA, Zhu M, Mizuno H et al (2001) Multilineage cells from human adipose tissue: implications for cell-based therapies. Tissue Eng 7:211–228